Adaptive Nonlinear Control of the Czochralski Process via Integration of Second Order Sliding Mode and Iterative Learning Control

Halima Zahra Bukhari[1], Muhammad Faisal Aftab[1], Jan Winkler[2] and Morten Hovd[1]

Abstract— **This paper utilises nonlinear second-order sliding mode (SOSM) combined with an iterative learning control (ILC) scheme for the control of interface dynamics primarily focused on diameter control in the Czochralski (CZ) process. The sliding mode control (SMC) or variable structure control (VSC) is well suited for systems with bounded and unstructured parametric uncertainties. The SOSM is therefore employed to attain robustness in the control despite unknown system dynamics. On the other hand, iterative learning control is incorporated as an intelligent module of the designed controller to better adapt to repetitive operation even in the presence of unknown parameters and bounded disturbances. Since CZ is a batch process that repeats itself every time a new crystal ingot is produced, repeatability renders learnability to the designed controller.**

Keywords: Iterative Learning Control, Second-order sliding mode, Czochralski Process, Parametric uncertainties, Interface dynamics.

I. Introduction

The Czochralski (CZ) process for growing single crystals of Si, Ge or GaAs is named after the polish scientist Jan Czochralski. In this paper we focus on the production of mono-crystalline silicon which is the fundamental material used in electronics and high efficiency photovoltaics. Automatic control of this process is essential to not only produce crystals with perfect lattice structure, but also to make its production cost effective through precise diameter control, thereby yielding minimal material cut off. For silicon wafers used for photovoltaics, the perfect crystal structure gives the highest light-to-electricity conversion efficiency.

The CZ process is a batch process with complex thermo-physical behavior. The complete model of this system includes dynamics of both interface geometry and temperature within the melt region. The interface geometry is greatly dependent upon heat and mass transfer across this region. This paper, however, employs control of interface dynamics only, thus implicitly, assuming steady state thermal conditions within the melt.

In a commercial CZ process, a mono-crystalline silicon ingot is pulled from the molten silicon while maintaining a controlled thermal environment inside the furnace. The prime objective is to achieve a constant diameter throughout the crystal body growth, despite thermal fluctuations/disturbances. The pulling speed v_p is manipulated to minimize diameter fluctuations thereby maintaining the crystal diameter within the desired range. The assembly for the silicon ingot production is shown in Figure 1.

The key crystal quality parameters of an Si ingot are not available during its production. However, it has been found that a controlled growth rate and constant crystal diameter during the production phase results in good quality of the produced ingot, i.e., a monocrystalline structure with few dislocations and and less material cut off.

The true system dynamics are highly complex and non-linear. Although complex dynamic models attempting to capture these complexities do exist, their use is limited to off-line simulation studies, as the lack of on-line measurements prohibits reliable updating of such models to actual operating conditions. In addition to above, the parameters of such mathematical models would be subject to wide variations owing to non uniform and unpredictable thermal conditions, wear and ageing of puller equipment and hot zone parts.

Traditionally, PID control is used in commercial CZ pullers, along with optimized feedforward trajectories for heater temperature control and mechanical pull speed, so as to minimize diameter fluctuations. A non-linear controller based on back-stepping has been proposed [1], but it requires the accurate knowledge of the plant dynamics that is not available.

The robust ILC design to compensate for the model errors and the repetitive external disturbances is a hot research topic. To address this, traditional ILC has been integrated with many well established control techniques like adaptive robust control, backstepping control, H_∞ control and sliding mode control.

In a nutshell, the changing system heat fluxes at the melt/crystal interface can be expressed as uncertainties in the system, which directly influence the crystallization process, thereby affecting the crystal diameter. These changing heat fluxes have a strong repetitive component, due to the repetitive nature of puller operation, and their effect on crystal diameter and pulling speed can therefore be learned by an ILC controller. In this paper, adaptive control approach based on second-order sliding mode (SOSM) and iterative learning control (ILC) is designed for diameter tracking in the CZ process. The motivation for adaptive control is to account for batch related variations in operating conditions as well as to compensate for slowly time-varying system parameters that are susceptible to changes owing to gradual system wear.

This paper is organized as follows: Section II outlines the dynamics of the CZ process, while the basics of ILC augmentation to second-order sliding mode control is discussed in Section III. The conversion of the system dynamics into

[1]Engineering Cybernetics Department, NTNU, Trondheim, Norway halima.bukhari@ntnu.no

[2]Institut für Regelungs- und Steuerungstheorie, Technische Universität, D-01062 Dresden, Germany.

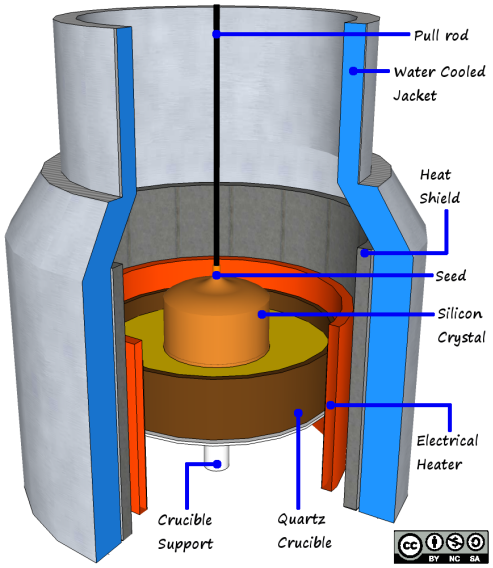

Fig. 1. Assembly of CZ puller. (This figure is licensed under a Creative-Commons BY-NC-SA license) [2].

the normal form, the control methodology followed by the simulation results are finally compiled in Section IV.

II. Melt/Crystal Interface Dynamics

A. Melt/crystal Interface Dynamics

Model based control techniques rely heavily on process models for characterization of dynamic relationships between controlled and manipulated variables. The process model in turn determines the choice of control structure to be used for the final controller design. For this study, only that part of the process model is considered, that describes the crystal geometric properties and hydromechanics at the interface. A sketch of the interface region is depicted in Figure 2 which shows important regimes in the crystallization process as well as the physical parameters reckoned essential for the subsequent study.

The crystal in contact with liquid-air interface causes meniscus formation. Its shape can be determined by numerically solving the famous *Young-Laplace* equation commonly used in capillary hydrodynamics. However, in many cases, an analytical approximation of the *Young-Laplace* equation can be used instead of its numerical solution. Many analytical approximations have been proposed in literature. The most widely used solution as derived by Boucher and Jones [3] algebraically relates crystal radius r_c and slope angle $\alpha_c := \alpha - \alpha_o$ with meniscus height h.

$$h = a\sqrt{\frac{1-sin(\alpha_0+\alpha_c)}{1+\frac{a}{\sqrt{2}r_c}}} \tag{1}$$

where a is Laplace's constant often referred to as capillary length, given as: $a = \sqrt{\gamma/\rho g}$. γ refers to the surface tension between melt and environment. As a result of (1) the geometric behavior of crystal growth can be characterized either through interface radius and meniscus height $(\dot{r_c}, \dot{h})$ or through interface radius and meniscus angle $(\dot{r_c}, \dot{\alpha_c})$ [4].

To achieve diameter control, the diameter of the bright ring formed on the meniscus is measured optically using a CCD camera. Based on the bright ring diameter measurement, the crystal diameter is estimated and the mechanical input, which in this case is the upward pull speed v_p of the ingot is continuously adjusted to achieve the diameter control.

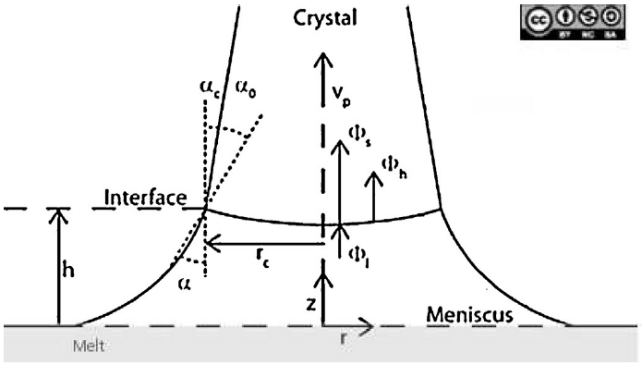

Fig. 2. Interface showing meniscus between melt and crystal (This figure is licensed under a Creative-Commons BY-NC-SA license) [2]

B. Hydrodynamical/Geometrical Interface Dynamics

The meniscus is produced as a result of gravitational forces and surface tension. Its upper end is the interface/phase boundary between molten and solid Si, where the crystallization takes place thereby releasing latent heat of fusion. Since the crystal is pulled upwards into colder regions of the furnace, a temperature gradient is established which leads to heat flow by conduction from the hot interface into the colder crystal. By this mechanism, crystallization is maintained throughout the growing process.

The overall hydromechanics at the interface are expressed in terms of system states ($\dot{r_c}$ and $\dot{\alpha_c}$) that are related mathematically through the following expressions [4]:

$$\begin{aligned} \dot{r_c} &= v_c tan(\alpha_c) \\ \dot{\alpha_c} &= \frac{v_p - v_{cru} - C_{\alpha,z} v_c}{C_{\alpha,n}} \end{aligned} \tag{2}$$

where v_{cru} is the crucible lifting rate, v_c is the crystal growth rate and the factors $C_{\alpha,z}$ and $C_{\alpha,n}$ are defined as:

$$\begin{aligned} C_{\alpha,z}(r_c,\alpha_c) = 1 - \frac{\rho_s r_c^2}{\rho_l r_{cru}^2} + \Bigg[\left(1-\frac{r_c^2}{r_{cru}^2}\right)\frac{\partial h}{\partial r_c} \\ - \frac{2r_c h}{r_{cru}^2} - \frac{a^2}{r_{cru}^2} cos(\alpha_0+\alpha_c)\Bigg] tan(\alpha_c) \end{aligned} \tag{3}$$

$$C_{\alpha,n}(r_c,\alpha_c) = \left(1-\frac{r_c^2}{r_{cru}^2}\right)\frac{\partial h}{\partial \alpha_c} + \frac{r_c a^2}{r_{cru}^2} sin(\alpha_0+\alpha_c) \tag{4}$$

where the growth angle $\alpha = \alpha_0 + \alpha_c$ is the angle between the line tangent to the meniscus surface at the melt-crystal interface and the lateral surface of the growing crystal. The angle α_c determines the growth direction and thereby the dynamics of the crystal diameter, whereas α_0 is the characteristic wetting angle of a specific material, i.e., 11°

in the case of Si. h is the height of tri-junction above the bulk melt, $u = v_p$ is the manipulated input, and v_c is the growth velocity normal to the interface and acting upwards in parallel to the direction of pull.

Finally, the crystal growth rate v_c is expressed as [4]:

$$\begin{aligned} v_c &= \frac{\Phi_s - \Phi_l}{A_i \rho_s \Delta H} = \frac{\phi_s - \phi_l}{\rho_s \Delta H} \\ &= \frac{1}{\rho_s \Delta H}\left(k_s \Delta T_s - k_l \Delta T_l\right) \end{aligned} \tag{5}$$

Here ρ_s is the density of the solid at melting point temperature, ΔH is the latent heat of fusion per unit volume, $k_{s,l}$ are thermal conductivities of crystal and melt respectively, A_i is the area of cross-section at the interface, $\Phi_l = k_l A_i \Delta T_l$ is the heat flow from the melt to the interface while $\Phi_s = k_s A_i \Delta T_s$ is the heat flow from the interface to the crystal. A necessary condition for growth is that the growth rate is positive, i.e. the heat flux/heat flow is directed from the melt into the crystal, i.e., ϕ_s is greater than ϕ_l. Otherwise, the sign of v_c reverses, thereby rendering the crystallization to stop and remelting the crystal. The two quantities $\phi_{s,l}$ are heat fluxes per unit area expressed in $[W/m^2]$.

III. Adaptive Learning Based on SOSM

The aim of this paper is to track the desired diameter trajectory in the presence of uncertainties due to variations in system parameters as well as unstructured uncertainties due to unmodeled system dynamics. The iterative learning control is widely employed for systems with repeatable operations. The system tracking response is improved iteratively through adaptive learning of variations in plant parameters combined with second order sliding mode control for robustness against unknown and unstructured uncertainties.

In literature the combined SOSM and ILC is referred to as Learning Variable Structure Control (LVSC), i.e., VSC and ILC are synthesized as the robust and intelligent parts respectively [5]. This LVSC control paradigm functions in two steps: First, VSC is designed to achieve the equivalent control profile that guarantees perfect tracking and complete disturbance rejection. Secondly, the iterative learning scheme is designed to learn the equivalent control repetitively based on tracking error signals from previous iterations. The VSC scheme can be viewed as the design of feedback control in parallel to the realization of feed forward control through ILC [5].

The higher order sliding mode techniques have been extensively investigated for the elimination of chattering effects encountered in traditional SMC. Furthermore, the designed control effort is continuous and more economical in restricting the system trajectory within the region of convergence. Consequently better robustness is achieved than with the traditional scheme despite the presence of noise and disturbances affecting the system.

A. Controller Design Strategy

The control scheme used in this paper is taken from the work by Ding *et. al* [6]. Consider the n^{th} order SISO nonlinear dynamical system with time-varying and uncertain parameters expressed in normal form as follows:

$$\begin{aligned} \dot{x}_{j,i} &= x_{j+1,i}, \quad 1 \le j \le n-1 \\ \dot{x}_{n,i} &= \boldsymbol{\theta}^T(t)\,\boldsymbol{\xi}(\boldsymbol{x}_i,t) + b(t)u_i(t) + d_i(t) \\ x_i(0) &= x_0, \quad t \in [0,T] \end{aligned} \tag{6}$$

where i is the iteration number that denotes the i^{th} repetitive operation of the system. $\boldsymbol{x}_i = [x_{1,i}, x_{2,i}, \ldots, x_{n,i}]^T \in \mathbb{R}^n$ and $u \in \mathbb{R}$ are the state vector and system input, respectively. $\boldsymbol{\theta}(t) \in C(\mathbb{R}^p, [0,T])$ is a vector of continuously differentiable unknown time-varying parameters, representing the parametric uncertainties, $b(t) \in C^1([0,T])$ is the unknown time-varying input gain and $d_i(t)$ denotes unknown bounded disturbance. $\boldsymbol{\xi}(\boldsymbol{x}_i,t) \in \mathbb{R}^p$ is a known vector function. The target trajectory is defined as $x_d(t) = [x_{1,d}(t), x_{2,d}(t), \ldots, x_{n,d}(t)]^T = [y_d(t), \dot{y}_d(t), \ldots, y_d^{(n-1)}(t)]^T$. The output vector is defined as the error signal between desired trajectory and the actual states, i.e., $e_i(t) = x_d(t) - x_i(t)$. The error term can be expanded as:

$$\begin{aligned} e_i(t) &= [e_{1,i}(t), e_{2,i}(t), \ldots, e_{n,i}(t)]^T \\ &= [y_d(t) - x_{1,i}(t), \dot{y}_d(t) - x_{2,i}(t), \ldots, y_d^{(n-1)}(t) - x_{n,i}(t)]^T \end{aligned}$$

The objective is to design a suitable control signal $u_i(t)$ such that the desired reference can be tracked with a small error tolerance ε as follows:

$$|x_d(t) - x(t)| \le \varepsilon$$

The following assumptions are imposed on the system for controller design:

Assumption 1: The initial resetting condition is satisfied, i.e., $e_i(0) = \dot{e}_i(0) = \ldots, e_i^{(n)}(0) = 0, \forall i$ and $t \in [0,T]$.

Assumption 2: The unknown disturbance is bounded such that: $|b^{-1}(t)\,d_i(t)| \le b_m \forall t \in [0,T]$, where b_m is a positive constant.

Assumption 3: The control direction of (6) is known, which implies that the sign of $b(t)$ is known for all $t \in [0,T]$.

B. Design of Sliding Manifold

The sliding surface dynamics can be expressed in terms of the error signal and its derivatives as follows:

$$\begin{aligned} \sigma_i(t) &= c_1 e_{1,i}(t) + c_2 e_{2,i}(t) + \ldots + c_n e_{n,i}(t) \\ &= \sum_{j=1}^{n} c_j e_{j,i}(t) = \sum_{j=1}^{n} c_j e_{1,i}^{(j-1)}(t) \end{aligned} \tag{7}$$

where the coefficient $c_n = 1$ and $c_j | j = 1, \ldots, n-1$ are the coefficients of a Hurwitz polynomial.

The derivatives of a sliding variable $\sigma_i(t)$ can be expressed as:

$$\begin{aligned} \dot{\sigma}_i(t) &= c_1 \dot{e}_{1,i}(t) + c_2 \dot{e}_{2,i}(t) + \ldots + \dot{e}_{n,i}(t) \\ &= c_1 e_{2,i}(t) + c_2 e_{3,i}(t) + \ldots + y_d^{(n)} - \dot{x}_{n,i} \\ &= \sum_{j=1}^{n-1} c_j e_{j+1,i}(t) + y_d^{(n)} \\ &\quad - \boldsymbol{\theta}^T(t)\,\boldsymbol{\xi}(\boldsymbol{x}_i,t) - b(t)u_i(t) - d_i(t) \end{aligned} \tag{8}$$

Consider a non-negative Lyapunov function at the i^{th} iteration as:

$$V_i(t) = \frac{\sigma_i^2(t)}{2b(t)} \tag{9}$$

The derivative of (9) is:

$$\begin{aligned}\dot{V}_i &= \frac{\sigma_i\dot{\sigma}_i}{b} - \frac{b^{-2}\dot{b}\sigma_i^2}{2} \\ &= \sigma_i\big[b^{-1}\sum_{j=1}^{n-1} c_j e_{j+1,i} - b^{-1}\boldsymbol{\theta}^T(t)\boldsymbol{\xi}(\boldsymbol{x}_i,t) \\ &+ b^{-1}y_d^{(n)} - u_i(t) - b^{-1}d_i(t) - \frac{1}{2}b^{-2}\dot{b}\sigma_i\big] \\ &= \sigma_i[\boldsymbol{\vartheta}^T\boldsymbol{\phi}_i - u_i(t) - b^{-1}d_i(t)]\end{aligned} \tag{10}$$

where $\boldsymbol{\vartheta} = [b^{-1}, -b^{-1}\boldsymbol{\theta}^T(t), b^{-2}\dot{b}]^T \in \mathbb{R}^{p+2}$ is the unknown time-varying system uncertainty and $\boldsymbol{\phi}_i = [y_d^{(n)} + \sum_{j=1}^{n-1} c_j e_{j+1,i}, \boldsymbol{\xi}^T, -\frac{1}{2}\sigma_i]^T \in \mathbb{R}^{p+2}$ is the known vector function.

Finally, the adaptive ILC based second-order sliding mode at the i^{th} iteration reads as:

$$\begin{aligned}u_i(t) &= k\sigma_i + \hat{\boldsymbol{\vartheta}}_i^T(t)\boldsymbol{\phi}_i - \upsilon_i(t) + \alpha|\sigma_i|^{\frac{2}{3}}sgn(\sigma_i) \\ \dot{\upsilon}_i(t) &= -\beta_1\sigma_i - \beta_2|\sigma_i|^{\frac{1}{3}}sgn(\sigma_i), \quad \upsilon_i(0) = 0 \\ \hat{\boldsymbol{\vartheta}}_i(t) &= \hat{\boldsymbol{\vartheta}}_{i-1}(t) + q\boldsymbol{\phi}_i(\eta|\sigma_i|^{\frac{1}{3}}sgn(\sigma_i) + \gamma\sigma_i), \quad \hat{\boldsymbol{\vartheta}}_{-1}(t) = 0\end{aligned} \tag{11}$$

where k is the feedback gain and q is the learning gain. The controller parameters α, β_1, β_2, γ and η are positive. The integral term $\upsilon_i(t)$ is used to cancel the effect of the unknown bounded disturbance. The expressions of $u_i(t)$ and $\upsilon_i(t)$ characterize the second order sliding mode and the expression of $\hat{\boldsymbol{\vartheta}}_i$ is the ILC law. The continuous functions $|\sigma_i|^{\frac{1}{3}}sgn(\sigma_i)$ and $|\sigma_i|^{\frac{2}{3}}sgn(\sigma_i)$ are used to reduce the control chattering effect.

Finally, for avid readers, the detailed convergence analysis based on composite energy functions for the adaptive ILC based second-order sliding mode control can be found in [6]. Similar analysis can also be found in [5],[7].

IV. Transformation to Normal Form, Controller Design and Simulation Results

The CZ dynamics of the interface has the same relative degree as the system order, i.e., n. Based on input-output linearization, the dynamics of (2) are transformed into the normal form by applying change of variables. The transformation of dynamics given by (2) into normal form is given in (12). For complete details, the reader may refer to [8],[9].

$$\begin{aligned}\dot{\zeta}_1 &= \zeta_2 \\ \dot{\zeta}_2 &= v_c\left[\frac{u - \left(v_{cru} + C_{\alpha,z}v_c\right)}{C_{\alpha,n}}\right] \\ &\quad sec^2\left(tan^{-1}\left(\frac{\zeta_2}{v_c}\right)\right)\end{aligned} \tag{12}$$

TABLE I

Thermo-physical properties of Si for the crystallization process

Ambient temperature, (T_{amb})	1262 K
Temperature at meniscus base, (T_B)	1690 K
Melting temperature, (T_M)	1685 K
Crystal density, (ρ_s)	2329 Kg/m^3
Melt density, (ρ_m)	2580 Kg/m^3
Crystal thermal conductivity, (k_s)	21.6 W/mK
Melt thermal conductivity, (k_l)	67.0 W/mK
Specific heat of fusion, (ΔH)	1.8e6 J/Kg
Crystal emissivity, (ε)	0.6
Stefan Boltzmann's Const. (κ)	5.67e-8 $W/(m^2.K^4)$
Surface tension (γ)	0.7835 N/m

TABLE II

Controller parameters

k	0.0125
c_1	0.1875
α	0.0125
β_1	0.0125
β_2	0.0125
γ	0.01875
q	0.01875
η	0.01875

V. Simulation Results

The designed second order sliding mode control integrated with the ILC has been tested in simulation studies for set point changes both in positive and negative directions. The thermo-physical parameters for the simulation tests are given in Table I. The initial conditions for diameter ($d = 2r$)) and the growth angle α are chosen to be $171mm$ and 0 respectively. The controller gains are listed in Table II. The peak (maximum) error (e_{max}) in each run has been chosen as the performance parameter. The simulation studies also show marked improvement in the transient response with each iteration. Two cases are presented here with 50mm change in diameter in both positive and negative sense. The reference trajectories are designed in such a manner that their smoothness up to first derivative are ensured.

A. Positive Set Point Change

The integrated sliding mode and iterative learning control is applied for 10 iterations. The peak error in each iteration is shown in Figure 4. It can be seen that after 10 iterations the maximum error has reduced by around 50 % as compared to the first iteration. The error plot given in Figure 3, shows the error profile for the 1^{st} run in blue that exhibits oscillatory behavior. The error profile for the 10^{th} iteration (black curve) shows marked improvement both in terms of transient response as well as tracking performance. The response to the positive 50mm set point change (10^{th} iteration) is shown in Figure 5 while the response for the meniscus height and the interface angle α, tends to a stable value as shown in Figure 6.

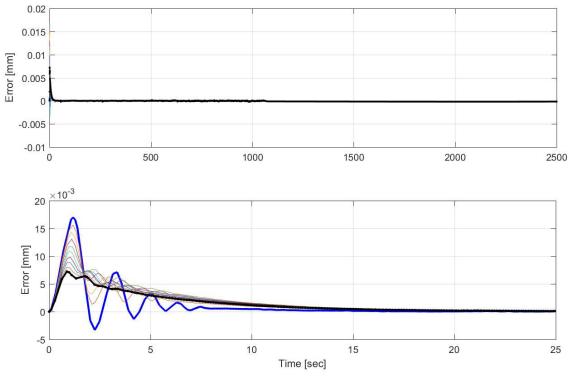

Fig. 3. Error signal for +50mm reference change : Black 10^{th} iteration; Blue 1^{st} iteration; zoomed view (second row)

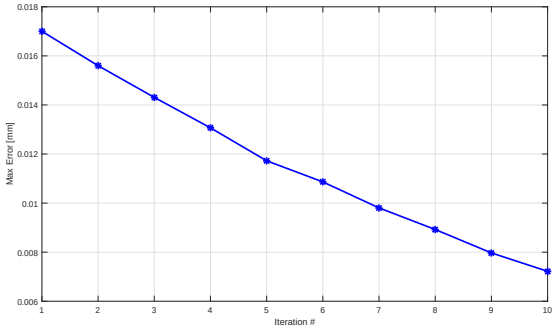

Fig. 4. Peak error in each iteration for positive set point change

B. Negative Set Point Change

The similar system response is exhibited for the set point change in the negative sense with peak error reduced up to 52% after ten iterations (Figure 8). The error curve given in Figure 7 shows marked improvement in the transient and tracking response (blue curve shows first iteration whereas black curve shows error for 10^{th} iteration). As in case for the positive set point change the meniscus height and interface angle tends to stable value (Figure 6).

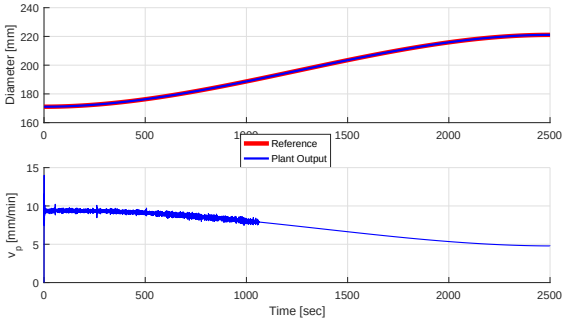

Fig. 5. Response for +50mm reference change (10^{th} iteration)

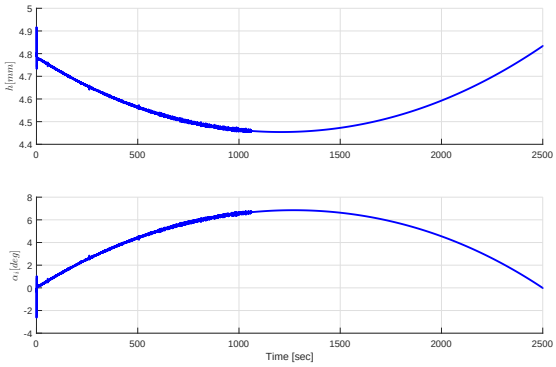

Fig. 6. Alpha and height response for positive set point change (10^{th} iteration)

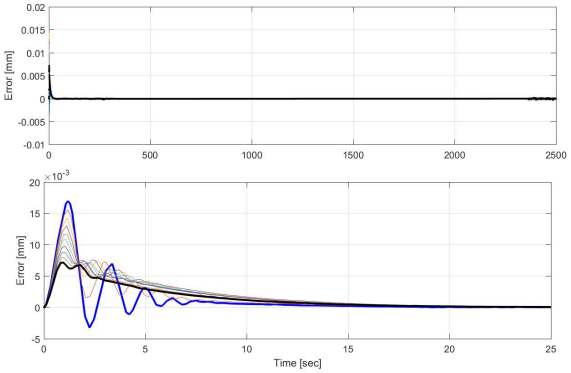

Fig. 7. Error signal negative 50mm reference change :: Black 10^{th} iteration; Blue 1^{st} iteration; zoomed view (second row)

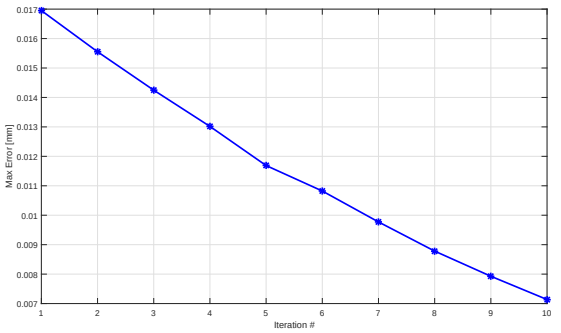

Fig. 8. Peak error in each iteration for negative set point change

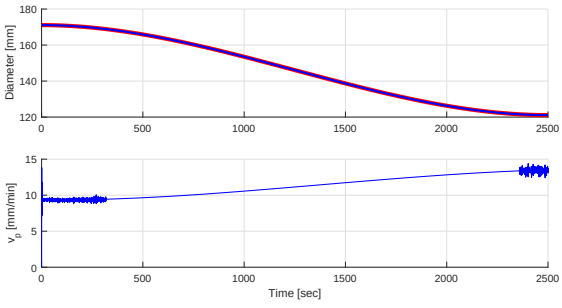

Fig. 9. Response for -50mm reference change (10^{th} iteration)

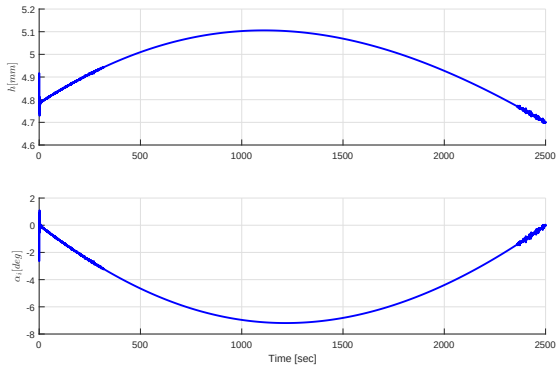

Fig. 10. Alpha and height response for negative set point change (10^{th} iteration)

VI. Conclusions

The crystal diameter control for the CZ interface dynamics using the ILC based SOSM control technique is presented in this paper. It is shown that the designed controller is able to track the commanded diameter quite well despite rough tuning of controller parameters. The simulation results show that with each subsequent iteration, the tracking error reduces thereby improving the system performance. This work can be further extended to real time implementation and design of non-linear observer for state estimation.

References

[1] P. Rahmanpour and M. Hovd, "Numerical backstepping for diameter control of silicon ingots in the czochralski process," in *Decision and Control (CDC), 2012 IEEE 51st Annual Conference on*. IEEE, 2012, pp. 7013–7017.

[2] P. Rahmanpour, S. Sælid, and M. Hovd, "Run-to-run control of the czochralski process," *Computers & Chemical Engineering*, vol. 104, pp. 353–365, 2017.

[3] E. A. Boucher and T. G. J. Jones, "Capillary phenomena. part 11.-approximate treatment of the shape and properties of fluid interfaces of infinite extent meeting solids in a gravitational field," *J. Chem. Soc., Faraday Trans. 1*, vol. 76, pp. 1419–1432, 1980. [Online]. Available: http://dx.doi.org/10.1039/F19807601419

[4] J. Winkler, M. Neubert, J. Rudolph, N. Duanmu, and M. Gevelber, "Czochralski process dynamics and control design," *Crystal growth processes based on capillarity: czochralski, floating zone, shaping and crucible techniques. Wiley, Chichester*, pp. 115–202, 2010.

[5] J.-X. Xu and W.-J. Cao, "Learning variable structure control approaches for repeatable tracking control tasks," *Automatica*, vol. 37, no. 7, pp. 997–1006, 2001.

[6] J. Ding and H. Yang, "Adaptive iterative learning control for a class of uncertain nonlinear systems with second-order sliding mode technique," *Circuits, Systems, and Signal Processing*, vol. 33, no. 6, pp. 1783–1797, 2014.

[7] W. Chen, Y.-Q. Chen, and C.-P. Yeh, "Robust iterative learning control via continuous sliding-mode technique with validation on an srv02 rotary plant," *Mechatronics*, vol. 22, no. 5, pp. 588–593, 2012.

[8] H. K. Khalil, *Nonlinear Systems*. Prentice-Hall, New Jersey, 1996.

[9] J.-J. E. Slotine, W. Li, *et al.*, *Applied nonlinear control*. prentice-Hall Englewood Cliffs, NJ, 1991, vol. 199, no. 1.